Journal of Catalysis 268 (2009) 196–200

Contents lists available at ScienceDirect

Journal of Catalysis

journal homepage: www.elsevier.com/locate/jcat

Fischer–Tropsch synthesis on a model Co/SiO_2 catalyst

Zhen Yan [a], Zhoujun Wang [a], Dragomir B. Bukur [b], D. Wayne Goodman [a,*]

[a] Department of Chemistry, Texas A&M University, College Station, TX 77843, United States
[b] Department of Chemical Engineering, Texas A&M University at Qatar, Doha, Qatar and Texas A&M University, College Station, TX 77843, United States

A R T I C L E I N F O

Article history:
Received 8 July 2009
Revised 7 September 2009
Accepted 22 September 2009
Available online 2 November 2009

Keywords:
Model catalyst
Cobalt catalyst
Silica
Fischer–Tropsch synthesis

A B S T R A C T

A model Co/SiO_2 catalyst was prepared by depositing cobalt on silica films in ultrahigh vacuum conditions. Fischer–Tropsch synthesis was carried out at a total pressure of carbon monoxide and hydrogen between 0.33 and 1.0 bar. The effects of reaction temperature and pressure on kinetics and chain growth probability were investigated. The turnover frequency, activation energy, and product distributions were found in good agreement with those obtained on real catalysts. The formation of cobalt oxide or cobalt carbide was not detected after Fischer–Tropsch reaction at the low conversions and low water partial pressures of this work.

1. Introduction

The world has seen the adverse effect caused by our dependence on crude oil, and much effort has been made to develop renewable energy technologies, such as solar, wind, and biofuels. However, it seems that none of these technologies can meet the huge energy requirements of our society. For example, in 2007, solar, wind, and biofuels combined only to contribute 1.5% of the energy consumption of USA [1]. On the other hand, the huge reserves of natural gas and coal exceed those of crude oil by factors of about 1.5 and 25, respectively [2]. Therefore, Fischer–Tropsch technology, although made vulnerable by the dramatic changes in crude oil prices, is still one of the few technologies that can replace oil in the future.

Supported cobalt catalysts have been extensively studied for Fischer–Tropsch synthesis (FTS) because of their higher activity compared to commercially used iron catalysts [2–7]. However, some fundamental questions remain controversial. For example, the oxidation of metallic cobalt to cobalt oxide or other cobalt compounds (such as cobalt silicate and cobalt aluminate) has been proposed to be a possible cause of deactivation for FTS on supported cobalt catalysts [8,9]. Kogelbauer et al. [9] reported the formation of cobalt silicates in Co/SiO_2 as determined by TPR following FTS (493–513 K, $P = 31$ bar, $H_2/CO = 2$). Similarly, Huber et al. [10] reported that Co/SiO_2 catalysts deactivated rapidly during FTS at high water partial pressures due to the formation of stable, inactive cobalt silicates. On the contrary, van de Loosdrecht et al. [11] studied the deactivation of an industrial Co/Al_2O_3 catalyst by X-ray diffraction, magnetic measurements and X-ray absorption near-edge spectroscopy, and the oxidation of cobalt was ruled out as a major deactivation mechanism.

FTS has also been studied using single crystal model catalysts. Structure sensitivity of FTS was observed on different surfaces of cobalt single crystals [12,13]. After reaction, longer chain hydrocarbon fragments were observed on the $Co(1 1 \bar{2} 0)$ surface, whereas on the stepped $(1 0 \bar{1} 2)$ and close-packed $(0 0 0 1)$ surfaces, mainly CH_x ($x = 1–3$) species were present on the surface. Beitel et al. [14] studied the co-adsorption of CO and H_2 on $Co(0 0 0 1)$ at pressures up to 300 mbar, and in situ polarization modulation reflection absorption infrared spectroscopy (PM-RAIRS) results suggested that defects were the active sites for hydrocarbon formation. Johnson et al. [15] reported that submonolayer cobalt deposited on $W(1 0 0)$ and $W(1 1 0)$ surfaces had similar activity for FTS, and the after-reaction AES spectra showed formation of carbidic species.

The model studies mentioned above were performed on metal single crystal surfaces. Real cobalt catalysts, on the other hand, are small metal particles supported on oxide materials, such as Al_2O_3, TiO_2 and SiO_2. Therefore, the conclusions drawn from these model studies may not apply to industrial applications. So far there have been very limited studies on oxide supported model catalysts. Saib et al. [16] studied the oxidation of a planar $Co/SiO_2/Si(1 0 0)$ model catalyst using in situ NEXAFS and found no surface oxidation of cobalt particles (4–5 nm) under model FTS conditions ($P_{Total} = 0.4$ mbar, 423–673 K).

In this study, a model Co/SiO_2 catalyst was prepared and studied under FTS conditions. The effects of reaction temperature and total pressure on FTS activity and product distribution were investigated, and the kinetic results were compared with those on real catalysts.

---

[*] Corresponding author. Fax: +1 979 845 6822.
E-mail address: goodman@mail.chem.tamu.edu (D.W. Goodman).

0021-9517/$ - see front matter © 2009 Elsevier Inc. All rights reserved.
doi:10.1016/j.jcat.2009.09.015

2. Experimental

The experiments were carried out in a modified commercial PHI 5500 system consisting of a surface analysis chamber, a preparation chamber, and a high-pressure cell. The surface analysis chamber, which is equipped with a dual Mg/Al anode X-ray source, a hemispherical energy analyzer, and a differential ion gun, allows the characterization and cleaning of catalyst samples. The stainless steel, high-pressure cell (0.2 L) is used as a batch reactor and separated from the preparation chamber by a gate valve, which allows other parts of the system to maintain ultrahigh vacuum (UHV) while Fischer–Tropsch synthesis is carried out in the reactor.

A tantalum foil (9 × 9 mm) was spot-welded to two tungsten wires mounted on a bellows manipulator, which allows translation of the sample to various positions. The sample was heated resistively and temperature was measured by a C-type thermocouple spot-welded to the back of the foil. SiO_2 films [17,18] were prepared by evaporating Si onto the Ta foil in a background of 1.3×10^{-8} bar oxygen, followed by annealing at 850 K. Cobalt was vapor-deposited on SiO_2 films from a cobalt wire wrapped with a tantalum filament, which was resistively heated. The Si and Co dosers were calibrated on a Mo(1 1 0) surface using XPS [19,20].

Carbon monoxide was first passed through an oxygen trap, and then a quartz tube, which was filled with quartz chips and kept at 573 K, to remove metal carbonyls. CO and H_2 with various ratios were premixed in an aluminum cylinder to ensure complete mixing. Before reaction, the H_2/CO mixtures were passed through a liquid-nitrogen trap before entering the reactor to remove other impurities. The products were analyzed with a HP 5890 gas chromatograph equipped with a flame ionization detector and a HP-PLOT Al_2O_3 capillary column. Blank experiments were carried out at various temperatures with clean tantalum foils and no reactions were observed at up to 573 K.

XPS spectra were collected using an Mg Kα X-ray source and a precision PHI hemispherical analyzer operated at a pass energy of 58.7 eV. The binding energies were referenced to the Si 2p line in SiO_2 at 103.4 eV.

3. Results and discussion

3.1. Activity and selectivity

The Co/SiO_2 model catalyst used in this study was prepared by depositing three equivalent monolayers of cobalt onto a 10 nm thick SiO_2 film, followed by annealing to 800 K in ultrahigh vacuum. The nominal Co/Si atomic ratio was 1:4, as estimated from the XPS peak areas and atomic sensitivity factors. The relative small Co/Si ratio suggests that cobalt was present as nanoparticles on the SiO_2 surface, instead of as continuous cobalt layers. In addition, the Co/Si XPS ratio decreased considerably after the annealing, indicating the sintering of cobalt particles. Other studies [16,21] by STM and AFM also showed that metals exist in the form of nanoparticles on amorphous silica films.

FTS was carried out on this catalyst at temperatures from 493 to 573 K using 1:1 H_2/CO mixtures at a total pressure of 1.0 bar. The products were mainly methane, ethylene, propylene, and butenes. A small amount of ethane and propane were also detected. For example, after an hour of reaction at 513 K, the concentrations of CH_4, C_2H_4, C_3H_6, and C_4H_8 were 20.7, 2.6, 1.8, and 0.8 ppm, respectively. The reaction rates, expressed as CO molecules converted per second, as a function of reaction time are shown in Fig. 1. The activity decreased in the first hour, particularly at higher temperatures, and then became relatively stable. The selectivities, on the other hand, did not show a similar steady state, as shown in Fig. 2 for the reaction at 513 K. The selectivity to C_2–C_4 products decreased almost linearly with time, as the CH_4 selectivity kept increasing. This suggests that the active sites for chain growth were poisoned by carbonaceous depositions, whereas the formation of methane on non-specific sites was not as affected [22].

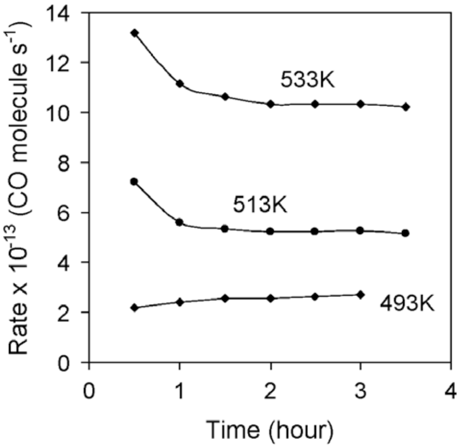

Fig. 1. FTS activity as a function of reaction time at various temperatures (1.0 bar, H_2/CO = 1).

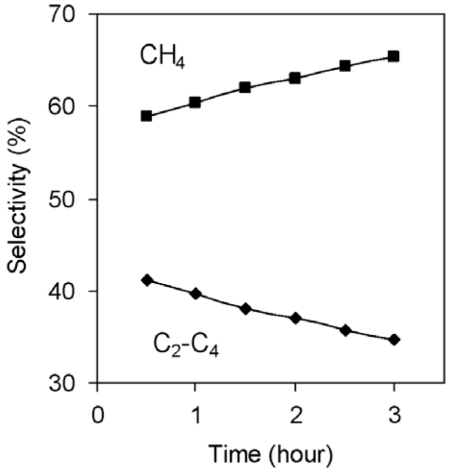

Fig. 2. Selectivity to CH_4 and C_2–C_4 products as a function of reaction time at 513 K, 1.0 bar, and H_2/CO = 1.

The Arrhenius plot of CO conversion rate (Fig. 3a) showed a straight line, giving an apparent activation energy of 93 kJ/mol. This value is consistent with the apparent activation energies of 93–103 kJ/mol from previous studies on cobalt-based FTS catalysts [23,24]. The formation rates of C_2–C_4 products apparently did not follow the Arrhenius law at higher temperature (>533 K), as shown in Fig. 3b, and their yields were lower than expected. This means that high temperature favors chain termination or desorption reactions since desorption is an endothermic process, so increasing temperature shifts selectivity to methane.

The reported turnover frequency of FTS (number of CO molecules per active site per second, or TOF) varies greatly in the literature. Recent studies [25,26] have shown that the TOF was strongly affected by cobalt particle sizes. More specifically, cobalt particles smaller than 6–8 nm were much less active than larger ones. Ribeiro et al. [27] reviewed kinetic studies of FTS and selected 36 sets of data on well-reduced cobalt catalysts from 12 different studies. The average TOF at 473 K, 10 bar, and H_2/CO = 2 was $0.017 \pm 0.014\ s^{-1}$. The reaction rate on our Co/SiO_2 catalyst was

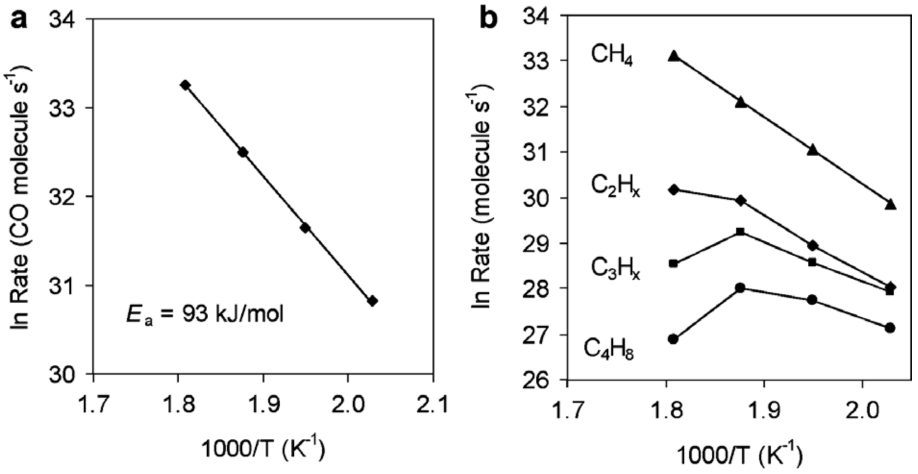

Fig. 3. Arrhenius plots of (a) CO conversion rate and (b) C_2–C_4 product formation rates at 1.0 bar and $H_2/CO = 1$.

9.18×10^{12} molecules s^{-1} at 473 K according to Fig. 3a, or 3.85×10^{13} molecules s^{-1} after correcting to 473 K, 10 bar, and $H_2/CO = 2$ using the power law equation ($r = kP_{H_2}^{0.7}P_{CO}^{-0.2}$) given by Ribeiro et al. Assuming that the number of active sites on the Co/SiO_2 catalyst equals the number of surface cobalt atoms on a Co(0 0 0 1) single crystal (1.84×10^{15} atoms/cm^2) with the same surface area, which is a reasonable estimate at high metal coverages [21], the TOF will be 0.026 s^{-1}, in good agreement with the average TOF above. The TOF is consistent with those reported by Bezemer et al. for cobalt particles larger than 6–8 nm [25].

Anderson–Schulz–Flory (ASF) plots are commonly used to characterize the product distribution of FTS [28]. Fig. 4 shows the ASF plots for the reactions at 493 and 553 K, where the molar concentrations were normalized such that the concentration of methane was unity. The chain growth probability or α was 0.55 at 493 K and 0.20 at 553 K. It was also observed at other reaction temperatures that the chain growth probability decreased with increasing temperature. This tendency is generally observed for FTS on supported catalysts [3]. For example, it was reported that α was 0.63 at 458 K and 0.52 at 484 K on a Co/Al_2O_3 catalyst [15]. It is noteworthy that methane deviated from the ASF plots, that is, more methane was produced than expected by the ASF distribution. In addition, less C_2 products were produced than expected, and this became more prominent at lower temperatures (533 K or lower).

Deviations of FTS products from ideal ASF distributions are often reported in the literature, particularly in low temperature FTS. The commonly observed deviations include a higher than expected methane content, lower than expected C_2 contents, and carbon number-dependent chain growth probability [3]. The excess formation of methane was explained by formation of additional methane on different sites that do not promote chain growth, or a contribution of hydrogenolysis [3,29]. Secondary reactions are often proposed as the most possible cause for the lower C_2 yield [30–32]. For example, residence time and olefin co-feeding studies on ruthenium catalysts [33] showed that readsorption of α-olefins and the resulting chain initiations were the most important secondary reactions and the deviations from ideal ASF distribution were ascribed to physical effects (i.e. carbon number dependent diffusivity or solubility). However, the probability of product readsorption was quite low in our study due to the low concentrations (e.g. <10 ppm for ethylene). It is not likely that olefin readsorption can make observable contributions to the product distribution. It is possible that ethylene stays longer on the surface than heavier olefins because it is geometrically more stable, and thus has a higher chain growth probability. The fact that the same deviations from the ASF distribution were observed in our study indicates that our model Co/SiO_2 catalyst is a good representation of supported FT catalysts.

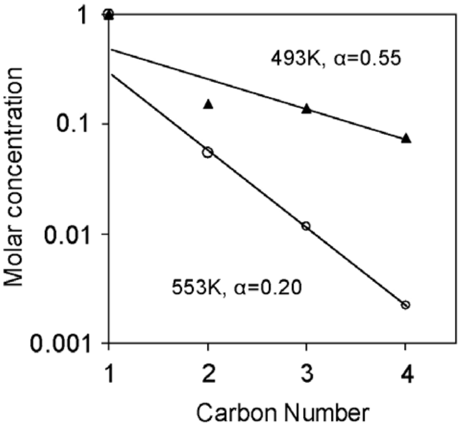

Fig. 4. ASF plots after 1 h reaction at 493 and 553 K, 1.0 bar, and $H_2/CO = 1$ (CH_4 was not included when calculating chain growth probability).

3.2. XPS results

Fig. 5 shows the cobalt 2p XPS spectra of the Co/SiO_2 catalyst acquired before and after FTS reaction (513 K, 3 h), as well as that of a CoO_x/SiO_2 surface prepared by oxidizing Co/SiO_2 at 700 K in 1.3×10^{-8} bar oxygen. The spectrum of CoO_x/SiO_2 shows prominent shake-up patterns that are characteristic of cobalt oxide. On the other hand, the absence of the shake-up satellites in the used Co/SiO_2 indicates that cobalt particles remained metallic after FTS reaction. FTS was also carried out on the oxidized CoO_x/SiO_2 as a comparison. The initial reaction rate on this surface was almost negligible; however, after an induction period of ~1 h, it showed activity similar to that of fresh Co/SiO_2. XPS results indicate that cobalt oxide was reduced to metallic cobalt after FTS.

The oxidation of cobalt particles during FTS was proposed by some researchers as a major cause of catalyst deactivation. Under our reaction conditions, the oxidation of cobalt was not observed; instead, cobalt oxide was reduced under FTS conditions. However, this does not rule out the possibility of cobalt oxidation as a cause of deactivation, because water vapor produced by FTS may play an important role in the oxidation of cobalt [10,34,35]. Due to the low conversions of CO and H_2 (<0.1%) in our study, the partial pressure of water was much lower than those in realistic FTS applications.

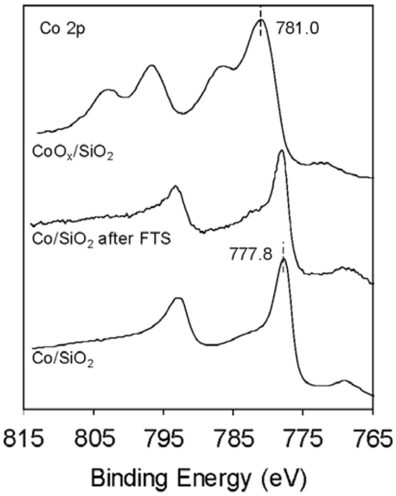

Fig. 5. Cobalt 2p XPS spectra of Co/SiO$_2$ before and after FTS (513 K, 1.0 bar, H$_2$/CO = 1), as well as that of oxidized CoO$_x$/SiO$_2$.

The carbon 1s XPS spectra of Co/SiO$_2$ before and after FTS are shown in Fig. 6. A strong peak at 284.6 eV after the reaction was mainly from hydrocarbon products adsorbed on the surface. The broadening of the C 1s peak at higher binding energy could be from carbon monoxide on the surface. The formation of surface carbides was proposed to be responsible for chain growth in FTS [36], or conversely cause catalyst deactivation [37]. The formation of cobalt carbide, which would give a C 1s peak at binding energy between 282 and 284 eV [38,39], was not observed in this study.

3.3. Effects of total pressure

FTS was carried out on the Co/SiO$_2$ model catalyst at various total pressures between 0.33 and 1 bar using 1:1 H$_2$/CO mixtures. Fig. 7 shows a logarithmic plot of the FTS activity at 513 K as a function of total pressure. The reaction rate increased linearly with the total pressure, giving an apparent reaction order of 0.54. Fierro et al. [40] reported a similar effect of total pressure on FTS activity on supported cobalt catalysts from 20 to 40 bar. Ribeiro et al. [27] found that a simple power law expression $r = kP_{H_2}^{0.7}P_{CO}^{-0.2}$ provided the best fit to 36 sets of kinetic data from 12 studies. When the partial pressures of CO and H$_2$ are equal, as in our study, the equation above becomes $r = kP_{Total}^{0.5}$, which is in very good agreement with our result.

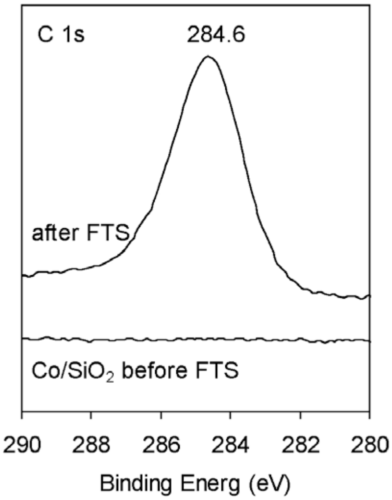

Fig. 6. Carbon 1s XPS spectra of Co/SiO$_2$ before and after FTS (513 K, 1.0 bar, H$_2$/CO = 1).

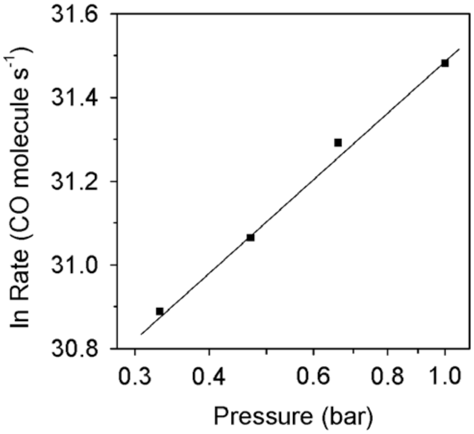

Fig. 7. Logarithms of the reaction rate as a function of total pressure at 513 K and H$_2$/CO = 1.

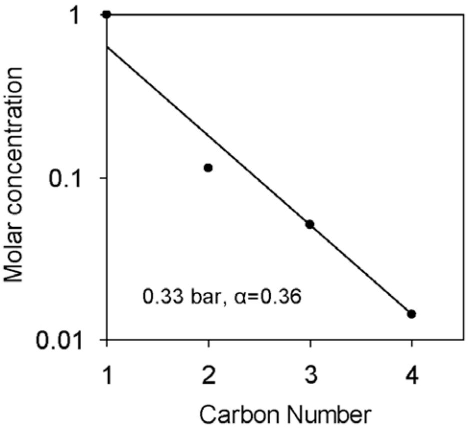

Fig. 8. ASF plot after 1 h reaction at 0.33 bar, 513 K, and H$_2$/CO = 1 (CH$_4$ was not included when calculating chain growth probability).

The deviations from ideal ASF plots were also observed at lower pressures (0.33–0.66 bar), similar to those observed at 1 bar. Figs. 8 and 9 shows the product distribution after the reaction at 0.33 bar and the chain growth probability as a function of total pressure.

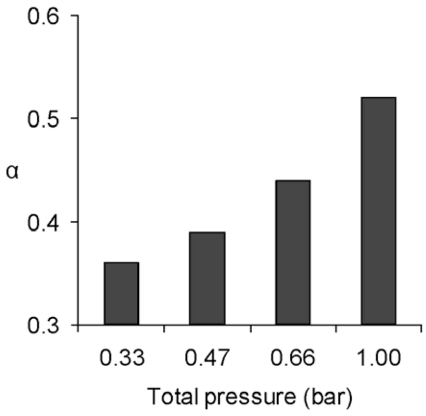

Fig. 9. Chain growth probability as a function of total pressure after FTS at 513 K and H$_2$/CO = 1.

The chain growth probability increased with increasing total pressure, indicating that high pressure favors selectivity to higher hydrocarbons. The beneficial effect of increasing operating pressure on FTS selectivity for cobalt-based catalysts has been reported in the literature [40,41]. Van Berge et al. [41] found that the chain growth probability increased with reactor pressure on a supported cobalt catalyst, whereas it was not affected by reactor pressure on an iron catalyst.

4. Conclusions

Fischer–Tropsch synthesis was carried out on a model Co/SiO_2 catalyst at various temperatures and pressures. Increasing reaction temperature raised the reaction rate but shifted the selectivity to methane. High pressures favored both the activity and the selectivity to longer hydrocarbons. The deactivation of catalyst was caused by carbonaceous depositions, and the formation of cobalt oxide or cobalt carbide was not observed after FTS. The turnover frequency, activation energy, effect of pressure, and product distributions were consistent with those obtained on real catalysts at much higher pressures (>10 bar) and different H_2/CO ratios. This indicates that our Co/SiO_2 catalyst is an ideal model for studying Fischer–Tropsch synthesis on supported cobalt catalysts.

Acknowledgments

This publication was made possible by a grant from the Qatar National Research Fund. This work was also partially supported by the Department of Energy, Office of Basic Energy Sciences, Division of Chemical Sciences, Geosciences, and Biosciences (DE-FG02-95ER-14511), and the Robert A. Welch Foundation.

References

[1] Energy Information Administration, US Department of Energy, Annual Energy Review 2007, Washington, DC, 2008.
[2] M.E. Dry, Catal. Today 71 (2002) 227.
[3] G. Van Der Laan, A. Beenackers, Catal. Rev. Sci. Eng. 41 (1999) 255.
[4] E. Iglesia, Appl. Catal. A 161 (1997) 59.
[5] A.A. Adesina, Appl. Catal. A 138 (1996) 345.
[6] A.Y. Khodakov, W. Chu, P. Fongarland, Chem. Rev. 107 (2007) 1692.
[7] B.H. Davis, Fuel Process. Technol. 71 (2001) 157.
[8] D. Schanke, A.M. Hilmen, E. Bergene, K. Kinnari, E. Rytter, E. Ådnanes, A. Holmen, Catal. Lett. 34 (1995) 269.
[9] A. Kogelbauer, J.C. Weber, J.G. Goodwin, Catal. Lett. 34 (1995) 259.
[10] G.W. Huber, C.G. Guymon, T.L. Conrad, B.C. Stephenson, C.H. Bartholomew, Stud. Surf. Sci. Catal. 139 (2001) 423.
[11] J. van de Loosdrecht, B. Balzhinimaev, J.A. Dalmon, J.W. Niemantsverdriet, S.V. Tsybulya, A.M. Saib, P.J. van Berge, J.L. Visagie, Catal. Today 123 (2007) 293.
[12] J.J.C. Geerlings, M.C. Zonnevylle, C.P.M. de Groot, Surf. Sci. 241 (1991) 302.
[13] J.J.C. Geerlings, M.C. Zonnevylle, C.P.M. de Groot, Surf. Sci. 241 (1991) 315.
[14] G.A. Beitel, C.P.M. de Groot, H. Oosterbeek, J.H. Wilson, J. Phys. Chem. B 101 (1997) 4035.
[15] B.G. Johnson, C.H. Bartholomew, D.W. Goodman, J. Catal. 128 (1991) 231.
[16] A.M. Saib, A. Borgna, J. van de Loosdrecht, P.J. van Berge, J.W. Niemantsverdriet, J. Phys. Chem. B 110 (2006) 8657.
[17] X. Xu, D.W. Goodman, Appl. Phys. Lett. 61 (1992) 774.
[18] X. Xu, D.W. Goodman, Surf. Sci. 282 (1993) 323.
[19] J.-W. He, X. Xu, J.S. Corneille, D.W. Goodman, Surf. Sci. 279 (1992) 119.
[20] J.-W. He, D.W. Goodman, Surf. Sci. 245 (1991) 29.
[21] S.M. McClure, M. Lundwall, F. Yang, Z. Zhou, D.W. Goodman, J. Phys. Chem. C 113 (2009) 9688.
[22] H. Schulz, Z. Nie, F. Ousmanov, Catal. Today 71 (2002) 351.
[23] I.C. Yates, C.N. Satterfield, Energy Fuels 5 (1991) 168.
[24] C.G. Cooper, T.-H. Nguyen, Y.-J. Lee, K.M. Hardiman, T. Safinski, F.P. Lucien, A.A. Adesina, Catal. Today 131 (2008) 255.
[25] G.L. Bezemer, J.H. Bitter, H.P.C.E. Kuipers, H. Oosterbeek, J.E. Holewijn, X. Xu, F. Kapteijn, A.J. van Dillen, K.P. de Jong, J. Am. Chem. Soc. 128 (2006) 3956.
[26] J.P. den Breejen, P.B. Radstake, G.L. Bezemer, J.H. Bitter, V. Frøseth, A. Holmen, K.P. de Jong, J. Am. Chem. Soc. 131 (2009) 7197.
[27] F.H. Ribeiro, A.E.S. Von Wittenau, C.H. Bartholomew, G.A. Somorjai, Catal. Rev. Sci. Eng. 39 (1997) 49.
[28] H. Schulz, Appl. Catal. A 186 (1999) 3.
[29] H. Schulz, E. vein Steen, M. Claeys, Stud. Surf. Sci. Catal. 81 (1994) 455.
[30] S. Novak, R.J. Madon, H. Suhl, J. Catal. 77 (1982) 141.
[31] D.S. Jordan, A.T. Bell, J. Phys. Chem. 90 (1986) 4797.
[32] H. Schulz, M. Claeys, Appl. Catal. A 186 (1999) 71.
[33] E. Iglesia, S.C. Reyes, R.J. Madon, J. Catal. 129 (1991) 238.
[34] P.J. van Berge, J. van de Loosdrecht, S. Barradas, A.M. van der Kraan, Catal. Today 58 (2000) 321.
[35] A.M. Hilmen, D. Schanke, K.F. Hanssen, A. Holmen, Appl. Catal. A 186 (1999) 169.
[36] R.C. Brady, R. Pettit, J. Am. Chem. Soc. 102 (1980) 6181.
[37] O. Ducreux, J. Lynch, B. Rebours, M. Roy, P. Chaumette, Stud. Surf. Sci. Catal. 119 (1998) 125.
[38] M.J. Ledoux, C.P. Huu, J. Guille, H. Dunlop, J. Catal. 134 (1992) 383.
[39] C.D. Wagner, W.M. Riggs, L.E. Davis, J.F. Moulder, G.E. Muilenberg, Handbook of X-ray Photoelectron Spectroscopy, Physical Electronics Division, Perkin–Elmer Corp., Eden Prairie, MN, 1979.
[40] V.A. de la Peña O'Shea, M.C. Alvarez-Galvan, J. Campos-Martin, J. Fierro, Catal. Lett. 100 (2005) 105.
[41] P.J. van Berge, R.C. Everson, Stud. Surf. Sci. Catal. 107 (1997) 207.